BB

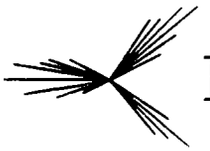

IFT

Instituto de Física Teórica
Universidade Estadual Paulista

May/95

IFT-P.024/95

Rho-omega mixing and the Nolen-Schiffer anomaly in relativistic nuclear models

L. A. Barreiro, A. P. Galeão and G. Krein

Instituto de Física Teórica
Universidade Estadual Paulista
Rua Pamplona 145
01405-900 - São Paulo, S.P.
Brazil

Instituto de Física Teórica
Universidade Estadual Paulista
Rua Pamplona, 145
01405-900 – São Paulo, S.P.
Brazil

Telephone: 55 (11) 251.5155
Telefax: 55 (11) 288.8224
Telex: 55 (11) 31870 UJMFBR
Electronic Address: LIBRARY@IFT.UESP.ANSP.BR
47553::LIBRARY

Rho-omega mixing and the Nolen-Schiffer anomaly in relativistic nuclear models

L. A. Barreiro, A. P. Galeão and G. Krein

Instituto de Física Teórica - Universidade Estadual Paulista

Rua Pamplona 145, 01405-900 São Paulo, SP, Brazil

Abstract

We calculate within the framework of relativistic nuclear models the contribution of the $\rho^0 - \omega$ mixing interaction to the binding energy differences of the mirror nuclei in the neighborhood of A=16 and A=40. We use two relativistic models for the nuclear structure, one with scalar and vector Woods-Saxon potentials, and the Walecka model. The ρ^0 - ω interaction is treated in first order perturbation theory. When using the Walecka model the ρ and ω nucleon coupling constants are the same for calculating bound state wave functions and the perturbation due to the mixing. We find that the relativistic results on the average are of the same order as the ones obtained with nonrelativistic calculations.

1 Introduction

The Nolen Schiffer anomaly (NSA) is the persistent discrepancy between experiment and conventional nuclear theory for the binding energy differences of mirror nuclei [1] [2]. From the studies along the last 25 years on the subject, there emerged a widespread consensus that the anomaly can eventually be explained by the charge symmetry violation in the nucleon-nucleon force [3]. In particular, class III (pp-nn) and class IV (pn) [4] charge symmetry breaking (CSB) forces can affect the binding energy differences of mirror nuclei [5]. In this context, Blunden and Iqbal [6] (BI) performed a systematic and detailed calculation of binding energy differences of mirror nuclei in the range of A = 11 to A = 41. In their calculation, BI employed CSB nucleon-nucleon potentials derived from $\rho^0 - \omega$ and $\pi^0 - \eta$ mixings and included the effects of the neutron-proton mass difference in the one- and two-pion exchange potentials. Within the framework of a Schrödinger equation calculation, using harmonic oscillator bound-state wave functions, BI concluded that CSB effects can resolve a large fraction of the anomaly. Moreover, their calculation showed that the ρ^0-ω mixing effect gives by far the most important contribution. In a subsequent calculation, Miller [7] obtained a larger effect than BI by using a new experimental value for the mixing parameter, which is larger than the one used by BI.

In this letter we calculate within the framework of two relativistic nuclear models the contribution of the $\rho^0 - \omega$ mixing interaction to the binding energy differences of the mirror nuclei in the neighborhood of A=16 and A=40. Both the nuclear structure and the mixing amplitude are treated relativistically. Relativistic models based on the original Walecka model [8] have been very successful in describing several nuclear properties and the study of CSB effects in the context of such models is an interesting new application. The only published calculation of binding energy differences of mirror nuclei using a relativistic nuclear model is the one by Nedjadi and Rook (NR) [9]. In their calculation the nuclear structure is described in a single-particle approximation in terms of the Dirac equation with scalar and vector Woods-Saxon potentials. The only CSB effects taken into account were the ones of the electromagnetic force. Here we calculate the binding energy differences employing the NR and Walecka models, both supplemented with the $\rho^0 - \omega$ mixing interaction. In the Walecka model we include the π, σ, ω, ρ, and the photon fields. In both models $\rho^0 - \omega$ mixing is treated in first order perturbation theory. In an earlier publication [10], the Walecka model was employed to calculate the contribution of the $\rho^0 - \omega$ mixing interaction to the neutron-proton self-energies in nuclear matter. The CSB effect found there is of the right sign and about the right magnitude of the anomaly in a large nucleus. The use of the Walecka model with the ρ^0 - ω mixing is particularly interesting because of the coupling coherence, i.e., the g_ρ and g_ω coupling constants appearing in the fundamental Lagrangian are the same for the nuclear structure and the CSB interaction. This is not the case for the NR model, where the nuclear structure has no direct connection with the CSB interaction.

We start with the NR model. In this model, the nuclear structure is described by the

single-particle Dirac equation with spherical mean fields:

$$\{-i\vec{\alpha}\cdot\nabla + \mathcal{W}(r) + \beta[M - U_s(r) - i\vec{\alpha}\cdot\nabla\mathcal{V}(r)]\}\,\mathcal{U}_\alpha(\vec{x}) = E_\alpha\mathcal{U}_\alpha(\vec{x})\,, \tag{1}$$

where $U_s(r)$ is a scalar potential, and the potentials $\mathcal{W}(r)$ and $\mathcal{V}(r)$ are given by:

$$\mathcal{W}(r) = U_v(r) + \frac{1}{2}(1+\tau_3)V_c(r)\,, \tag{2}$$

$$\mathcal{V}(r) = \left[\frac{\kappa_p}{2M}\frac{(1+\tau_3)}{2} + \frac{\kappa_n}{2M}\frac{(1-\tau_3)}{2}\right]V_c(r)\,, \tag{3}$$

$U_v(r)$ is a vector potential and $V_c(r)$ is the Coulomb potential. The term $\vec{\alpha}\cdot\nabla\mathcal{V}(r)$, which is due to the anomalous magnetic moments of the proton and the neutron, was not included in the Dirac equation of Ref. [9]. The index $\alpha = \{a,m\} = \{n,\kappa,m,t\}$ indicates the usual quantum numbers of energy (n), Dirac (κ), total angular momentum projection (m) and isospin projection (t). In the NR model, the scalar and vector potentials U_s and U_v are parametrized in terms of Woods-Saxon forms:

$$U_i(r) = \frac{V_i}{1+e^{(r-R_i)/a_i}}\,, \qquad i = v,s\,. \tag{4}$$

The parameters V_i, R_i, and a_i are adjusted to give the best fit to the single particles levels of the nuclei of interest.

The single-particle spinors $\mathcal{U}_\alpha(\vec{x})$ are written as usually:

$$\mathcal{U}_\alpha(\vec{x}) = \frac{1}{r}\begin{pmatrix} iG_{n\kappa t}\Phi_{\kappa m} \\ -F_{n\kappa t}\Phi_{-\kappa m}\end{pmatrix}\zeta_t\,, \tag{5}$$

where κ is the Dirac quantum number given in terms of the total angular momentum as

$$j = |\,\kappa\,| - \frac{1}{2}\,, \tag{6}$$

and

$$\Phi_{\kappa m} = \sum_{m_l m_s}(lm_l\tfrac{1}{2}m_s\,|\,l\tfrac{1}{2}jm)Y_{lm_l}(\theta\phi)\xi_{m_s}\,, \tag{7}$$

with

$$l = \begin{cases}\kappa & \kappa > 0\\ -(\kappa+1) & \kappa < 0\,,\end{cases}$$

and ξ_{m_s} and ζ_t are respectively Pauli spin and isospin spinors.

The components G and F are solutions of the following set of coupled first order equations:

$$\left(\frac{d}{dr} - \frac{\kappa}{r} + \frac{d\mathcal{V}(r)}{dr}\right)F_{n\kappa t}(r) + [E_{n\kappa t} - \mathcal{W}(r) - M + U_s(r)]\,G_{n\kappa t}(r) = 0\,, \tag{8}$$

$$\left(\frac{d}{dr} + \frac{\kappa}{r} - \frac{d\mathcal{V}(r)}{dr}\right)G_{n\kappa t}(r) - [E_{n\kappa t} - \mathcal{W} + M - U_s(r)]\,F_{n\kappa t}(r) = 0\,. \tag{9}$$

We solved these coupled Dirac equations in two ways: (1) directly, using the method of Ref. [11], and (2) by transforming the two first order equations into a second order Schrödinger equivalent equation as in Ref. [9]. Both methods gave the same results. We fixed the parameters of the Woods Saxon potentials to get the best fit to the single-particle energies and r.m.s. charge radii; these are:

$$\begin{aligned} V_s &= -473.5\ \text{MeV}, \quad R_s = 3.9\ \text{fm}, \quad a_s = 0.6\ \text{fm},\\ V_v^0 &= 398.5\ \text{MeV}, \quad R_v = 3.9\ \text{fm}, \quad a_v = 0.6\ \text{fm}. \end{aligned} \tag{10}$$

for ^{16}O, and

$$\begin{aligned} V_s &= -457.2\ \text{MeV}, \quad R_s = 3.95\ \text{fm}, \quad a_s = 0.8\ \text{fm},\\ V_v^0 &= 378.5\ \text{MeV}, \quad R_v = 3.95\ \text{fm}, \quad a_v = 0.8\ \text{fm}. \end{aligned} \tag{11}$$

for ^{40}Ca. For $V_c(r)$ we used the same of Nedjadi and Rook, namely the Coulomb potential corresponding to a uniformly charged sphere of radius $R_c = 1.25A^{1/3}$ fm. The results for the single-particle energies, $\epsilon_a = E_a - M$, and r.m.s. charge radii are shown in Table 1 below. The corresponding experimental values shown in column Exp for ^{16}O are taken from Ref. [12] and the ones for ^{40}Ca are taken from Ref. [13].

The other model we use for the nuclear structure is the one originally introduced by Walecka [8], supplemented by the $\pi-$ and $\rho-$meson and photon fields. We also include the tensor couplings of the photon and vector mesons. The Lagrangian density of the model is given by:

$$
\begin{aligned}
\mathcal{L} &= \bar{\psi}\left\{\gamma_\mu\left[i\partial^\mu - g_\omega\omega^\mu - \frac{f_\pi}{m_\pi}\gamma_5\boldsymbol{\tau}\cdot\partial^\mu\boldsymbol{\pi} - g_\rho\boldsymbol{\tau}\cdot\boldsymbol{\rho}^\mu - e\frac{1}{2}(1+\tau_3)A^\mu\right] - (M - g_s\phi)\right\}\psi \\
&+ \frac{1}{2}\left(\partial_\mu\phi\partial^\mu\phi - m_s^2\phi^2\right) + \frac{1}{2}\left(\partial_\mu\boldsymbol{\pi}\cdot\partial^\mu\boldsymbol{\pi} - m_\pi^2\boldsymbol{\pi}\cdot\boldsymbol{\pi}\right) - \frac{1}{4}F_{\mu\nu}F^{\mu\nu} \\
&- \frac{1}{2}\left(\frac{1}{2}G_{\mu\nu}G^{\mu\nu} - m_\omega^2\omega_\mu\omega^\mu\right) - \frac{1}{2}\left(\frac{1}{2}\mathbf{B}_{\mu\nu}\cdot\mathbf{B}^{\mu\nu} - m_\rho^2\boldsymbol{\rho}_\mu\cdot\boldsymbol{\rho}^\mu\right) \\
&- i\frac{1}{2}e\frac{\kappa_p}{2M}F_{\mu\nu}\bar{\psi}\frac{1}{2}(1+\tau_3)\gamma^\mu\gamma^\nu\psi - i\frac{1}{2}e\frac{\kappa_n}{2M}F_{\mu\nu}\bar{\psi}\frac{1}{2}(1-\tau_3)\gamma^\mu\gamma^\nu\psi \\
&- i\frac{1}{2}g_\omega\frac{\kappa_\omega}{2M}G_{\mu\nu}\bar{\psi}\gamma^\mu\gamma^\nu\psi - i\frac{1}{2}g_\rho\frac{\kappa_\rho}{2M}B^3_{\mu\nu}\bar{\psi}\tau_3\gamma^\mu\gamma^\nu\psi \\
&- e\left[\boldsymbol{\rho}_\nu\wedge\mathbf{B}^{\nu\mu} + \boldsymbol{\pi}\wedge(\partial^\mu\boldsymbol{\pi} + g_\rho\boldsymbol{\pi}\wedge\boldsymbol{\rho}^\mu)\right]_3 A_\mu + \mathcal{L}_{\rho^0-\omega}\,, \qquad (12)
\end{aligned}
$$

where, ψ, A^μ, ϕ, $\boldsymbol{\pi}$, ω^μ, and $\boldsymbol{\rho}^\mu$ are respectively the nucleon, photon, scalar isoscalar, pseudoscalar-isovector, vector-isoscalar and vector-isovector meson fields, and $F^{\mu\nu}$, $G^{\mu\nu}$, and $\mathbf{B}^{\mu\nu}$ are the vector field tensors defined in the usual way, $F^{\mu\nu} = \partial^\mu A^\nu - \partial^\nu A^\mu$, $G^{\mu\nu} = \partial^\mu V^\nu - \partial^\nu V^\mu$, $\mathbf{B}^{\mu\nu} = \partial^\mu\boldsymbol{\rho}^\nu - \partial^\nu\boldsymbol{\rho}^\mu$. The $\rho^0-\omega$ mixing Lagrangian density $\mathcal{L}_{\rho^0-\omega}$ can be written as:

$$
\mathcal{L}_{\rho^0-\omega} = \lambda\omega^\mu\rho_\mu^0\,, \qquad (13)
$$

where $\lambda \equiv -2m_\rho <\omega|H|\rho^0>$, is the ρ^0-ω mixing parameter.

We solve the model in the Hartree-Fock approximation [14]. However, below we present the Hartree formulae only because the complete expressions with the Fock terms are too lengthy to be presented in this letter; the complete expressions will be presented elsewhere. The coupled first order equations for the upper and lower components F and G are the same as in Eqs. (8,9), and the potentials $\mathcal{W}$ and $\mathcal{V}$ are now given by:

$$
\mathcal{W}(r) = g_\omega\omega_0(r) + g_\rho\tau_3\rho_0^0(r) + e\frac{1}{2}(1+\tau_3)A_0(r)\,, \qquad (14)
$$

$$
\mathcal{V}(r) = e\left[\frac{\kappa_p}{2M}\frac{(1+\tau_3)}{2} + \frac{\kappa_n}{2M}\frac{(1-\tau_3)}{2}\right]A_0(r) + g_\omega\frac{\kappa_\omega}{2M}\omega_0(r) + g_\rho\frac{\kappa_\rho}{2M}\tau_3\rho_0^0(r)\,. \qquad (15)
$$

The potentials $\phi_0(r)$, $\omega_0(r)$, $\rho_0^0(r)$, and $A_0(r)$ are not given external functions, but are determined self-consistently. They are given by integrals over the nucleon source terms, which depend on the F and G functions. Because of the tensor couplings, the source

terms for the vector fields are modified as compared to the usual ones [8]; they are given by:

$$
\begin{aligned}
\omega_0(r) = &- g_\omega\int_0^\infty dr'\,r'^2\Delta(r,r';m_\omega)\sum_{n\kappa t}^{occ}\left(\frac{2j_\kappa+1}{4\pi r'^2}\right)\Big\{\left[|\,G_{n\kappa t}(r')\,|^2 + |\,F_{n\kappa t}(r')\,|^2\right] \\
&- \frac{\kappa_\omega}{2M}(-2)\frac{d}{dr'}[G_{n\kappa t}(r')F_{n\kappa t}(r')]\Big\}\,, \qquad (16)
\end{aligned}
$$

$$
\begin{aligned}
\rho_0^0(r) = &- g_\rho\int_0^\infty dr'\,r'^2\Delta(r,r';m_\rho)\sum_{n\kappa t}^{occ}\left(\frac{2j_\kappa+1}{4\pi r'^2}\right)2t\Big\{\left[|\,G_{n\kappa t}(r')\,|^2 + |\,F_{n\kappa t}(r')\,|^2\right] \\
&- \frac{\kappa_\rho}{2M}(-2)\frac{d}{dr'}[G_{n\kappa t}(r')F_{n\kappa t}(r')]\Big\}\,, \qquad (17)
\end{aligned}
$$

and

$$
\begin{aligned}
A_0(r) = &- e\int_0^\infty dr'\,r'^2\Delta(r,r';0)\sum_{n\kappa t}^{occ}\left(\frac{2j_\kappa+1}{4\pi r'^2}\right)\Big\{\left[|\,G_{n\kappa t}(r')\,|^2 + |\,F_{n\kappa t}(r')\,|^2\right]\left(\frac{1}{2}+t\right) \\
&- \left[\frac{\kappa_p}{2M}\left(\frac{1}{2}+t\right) + \frac{\kappa_n}{2M}\left(\frac{1}{2}-t\right)\right](-2)\frac{d}{dr'}[G_{n\kappa t}(r')F_{n\kappa t}(r')]\Big\} \qquad (18)
\end{aligned}
$$

where $\Delta(r,r',m)$ is the Green's function

$$
\Delta(r,r',m_i) = -\frac{1}{m_i r r'}\sinh(m_i r_<)\exp(-m_i r_>), \qquad (19)
$$

with $r_>$ ($r_<$) being the greatest (smallest) between r and r'.

The parameters of the model are the masses and the coupling constants. For the pion parameters we take the ones used in the Bonn potential [15]. The parameters of the other mesons are usually chosen to adjust the saturation properties of nuclear matter [16]. Although the single-particle levels and r.m.s. charge radii for both ^{16}O and ^{40}Ca nuclei with such a set of parameters come out in reasonable accord with the experimental values [16], we preferred to readjust the parameters to get the best fit of the spectra and radii. We used the following set of parameters: $g_\sigma^2 = 113.6$, $g_\omega^2 = 195.2$ for ^{16}O and $g_\sigma^2 = 115.8$, $g_\omega^2 = 201.1$ for ^{40}Ca and $g_\rho^2 = 16.3$ for both nuclei. The final results for the binding energy differences are not affected by this readjustment in a significant way. For the anomalous couplings we used $\kappa_p = 1.79$, $\kappa_n = -1.91$, $\kappa_\omega = -0.12$, and $\kappa_\rho = 3.7$.

The results are shown in Table 2. Columns H and HF are respectively the Hartree and Hartree-Fock results. In both columns the tensor couplings have been neglected. Column

T presents the Hartree result including the tensor couplings. From this column one sees that the effect of the tensor couplings on the binding energies is not significant. One also notices that there is no significant difference between the Hartree and Hartree-Fock results.

The next step is to evaluate in first order perturbation theory the effect of the $\rho^0 - \omega$ mixing interaction on the binding energy differences. The binding energy difference between two mirror nuclei can be written as:

$$\Delta E = E_0(A \pm p) - E_0(A \pm n) \ , \tag{20}$$

where $E_0(A \pm p)$ and $E_0(A \pm n)$ are respectively the ground state energies of nuclei with A nucleons plus (minus) one proton and A nucleons plus (minus) one neutron. We are interested in the contribution from the $\rho^0 - \omega$ mixing interaction to ΔE. In first order this is:

$$\begin{aligned} \Delta E_{\rho\omega} &\equiv < A \pm p|H_{\rho\omega}|A \pm p> - < A \pm n|H_{\rho\omega}|A \pm n > \\ &= \pm \sum_{\alpha=1}^{A} (<\alpha p|H_{\rho\omega}|\alpha p> - <\alpha n|H_{\rho\omega}|\alpha n>) \ , \end{aligned} \tag{21}$$

where the perturbation $H_{\rho\omega}$ is, from Eq. (13), given by

$$H_{\rho\omega} = \int d^3x \ \mathcal{H}_{\rho\omega} = -\lambda \int d^3x \ : \omega^\mu(x)\rho^0_\mu(x) : \ , \tag{22}$$

and $|A \pm p>$ and $|A \pm n>$ are the ground state nuclei.

$\Delta E_{\rho\omega}$ requires evaluation of two-nucleon matrix elements of the type $< \xi\eta|H_{\rho\omega}|\xi\eta >$ where ξ, η=p, n. First, we write the solutions for the ω_μ and ρ^0_μ fields in terms of the nucleon densities as

$$\omega_\mu(x) = \int d^4y \ D^\omega_{\mu\nu}(x-y) \left[g_\omega \bar{\psi}(y)\gamma^\nu\psi(y) + \frac{\kappa_\omega}{2M}\partial_\lambda\psi(y)\sigma^{\lambda\nu}\psi(y) \right] \ , \tag{23}$$

$$\rho^0_\mu(x) = \int d^4y \ D^\rho_{\mu\nu}(x-y) \left[g_\rho \bar{\psi}(y)\gamma^\nu\tau_3\psi(y) + \frac{\kappa_\rho}{2M}\partial_\lambda\psi(y)\sigma^{\lambda\nu}\tau_3\psi(y) \right] \ , \tag{24}$$

where the $D^\omega_{\mu\nu}$ and $D^\rho_{\mu\nu}$ are the Green's functions of respectively the ω and ρ^0 field equations.

Neglecting antiparticles, the nucleon field operator can be expanded as:

$$\psi(x) = \sum_\alpha \mathcal{U}_\alpha(\mathbf{x}) e^{-iE_\alpha x_0} A_\alpha \ , \tag{25}$$

where A_α ($A^\dagger_\alpha$) is the nucleon annihilation (creation) operator, and $\mathcal{U}_\alpha(\mathbf{x})$ are given in Eq. (5). Then, substituting Eqs. (23,24) in Eq. (22) and using for the nucleon field operator the expansion above, we obtain for $H_{\rho\omega}$ the following expression:

$$\begin{aligned} H_{\rho\omega} &= -\frac{\lambda}{m^2_\omega - m^2_\rho} \int d^3x \ d^4y \int \frac{d^4k}{(2\pi)^2} \left[D^\omega_{\mu\nu}(k) - D^\rho_{\mu\nu}(k) \right] e^{ik(x-y)} \\ &\times \sum_{\alpha\beta\gamma\delta} e^{i(\epsilon_\alpha - \epsilon_\delta)y_0} \left[\mathcal{U}_\alpha(\mathbf{x}) \left(g_\omega\gamma^\mu + i\frac{\kappa_\omega}{2M}k_\lambda\sigma^{\lambda\mu} \right) \mathcal{U}_\beta(\mathbf{x}) \right] \\ &\cdot \left[\mathcal{U}_\gamma(\mathbf{y}) \left(g_\rho\gamma^\nu + i\frac{\kappa_\rho}{2M}k_\lambda\sigma^{\lambda\nu} \right) \tau_3 \mathcal{U}_\delta(\mathbf{y}) \right] A^\dagger_\alpha A^\dagger_\gamma A_\gamma A_\beta \end{aligned} \tag{26}$$

One can perform the integral over over y_0 and k_0 to obtain:

$$\begin{aligned} H_{\rho\omega} &= -\frac{\lambda g_\rho g_\omega}{m^2_\omega - m^2_\rho} \int d^3x \ d^3y \int \frac{d^3k}{(2\pi)^3} \left[D_{\mu\nu}(\epsilon_\beta - \epsilon_\alpha, \mathbf{k}) - D_{\mu\nu}(\epsilon_\gamma - \epsilon_\delta, \mathbf{k}) \right] \\ &\cdot e^{-i\mathbf{k}\cdot(\mathbf{x}-\mathbf{y})} \sum_{\alpha\beta\gamma\delta} \left\{ \left[\mathcal{U}_\alpha(\mathbf{x})\gamma^\mu\mathcal{U}_\beta(\mathbf{x}) \right] \left[\mathcal{U}_\gamma(\mathbf{y})\gamma^\nu\mathcal{U}_\delta(\mathbf{y}) \right] \right. \\ &+ \frac{\kappa_\omega}{2M}\frac{\kappa_\rho}{2M}(\epsilon_\beta - \epsilon_\alpha)^2 \left[\mathcal{U}_\alpha(\mathbf{x})\sigma^{0\mu}\mathcal{U}_\beta(\mathbf{x}) \right] \left[\mathcal{U}_\gamma(\mathbf{y})\sigma^{0\nu}\tau_3\mathcal{U}_\delta(\mathbf{y}) \right] \\ &- \frac{\kappa_\omega}{2M}\frac{\kappa_\rho}{2M}k^i k^j \left[\mathcal{U}_\alpha(\mathbf{x})\sigma^{i\mu}\mathcal{U}_\beta(\mathbf{x}) \right] \left[\mathcal{U}_\gamma(\mathbf{y})\sigma^{j\nu}\tau_3\mathcal{U}_\delta(\mathbf{y}) \right] \\ &- i\frac{\kappa_\rho}{2M}k^i \left[\mathcal{U}_\alpha(\mathbf{x})\gamma^\mu\mathcal{U}_\beta(\mathbf{x}) \right] \left[\mathcal{U}_\gamma(\mathbf{y})\sigma^{i\nu}\tau_3\mathcal{U}_\delta(\mathbf{y}) \right] \\ &\left. - i\frac{\kappa_\omega}{2M}k^i \left[\mathcal{U}_\alpha(\mathbf{x})\sigma^{i\mu}\mathcal{U}_\beta(\mathbf{x}) \right] \left[\mathcal{U}_\gamma(\mathbf{y})\gamma^\nu\tau_3\mathcal{U}_\delta(\mathbf{y}) \right] \right\} A^\dagger_\alpha A^\dagger_\gamma A_\gamma A_\beta \end{aligned} \tag{27}$$

The integrations over d^3k and the angles of $\mathbf{x}$ and $\mathbf{y}$ can be done analytically. The resulting expressions, with all the tensor couplings included, are very lenghty and not very instructive. For illustrative purposes we present the results with the tensor couplings dropped (the numerical results of Table 2 do include their effects). These can be written in terms of two functions $I_{\alpha\beta\gamma\delta}(r,r')$ and $J_{\alpha\beta\gamma\delta}(r,r')$, which result from integrals of terms respectively proportional to $\left[\Phi^\dagger_\alpha\Phi_\beta\right]\left[\Phi^\dagger_\gamma\Phi_\delta\right]$ and $\left[\Phi^\dagger_\alpha\boldsymbol{\sigma}\Phi_\beta\right]\cdot\left[\Phi^\dagger_\gamma\boldsymbol{\sigma}\Phi_\delta\right]$. They are given by:

$$I_{\alpha\beta\gamma\delta}(r,r') = \frac{1}{2\pi^2}\sum_l (2l+1)(-1)^{m_\alpha - m_\beta + j_\alpha + j_\gamma + l_\alpha + l_\gamma + 1} \left[I^{(\omega)}_{\alpha\beta l}(r,r') - I^{(\rho)}_{\alpha\beta l}(r,r') \right]$$

$$\times\ [(2l_\alpha+1)(2j_\beta+1)(2l_\gamma+1)(2j_\delta+1)]^{\frac{1}{2}}\,\langle l_\alpha 0 l 0 \mid l_\alpha l l_\beta 0\rangle\langle l_\gamma 0 l 0 \mid l_\gamma l l_\delta 0\rangle$$

$$\times\ \langle l m_\alpha - m_\beta j_\beta m_\beta \mid l j_\beta j_\alpha m_\alpha\rangle\langle l m_\alpha - m_\beta j_\delta m_\delta \mid l j_\delta j_\gamma m_\gamma\rangle$$

$$\times\ \begin{Bmatrix} l_\alpha & j_\alpha & \frac{1}{2} \\ j_\beta & l_\beta & l \end{Bmatrix} \begin{Bmatrix} l_\gamma & j_\gamma & \frac{1}{2} \\ j_\delta & l_\delta & l \end{Bmatrix}, \tag{28}$$

and

$$J_{\alpha\beta\gamma\delta}(r,r') = \frac{3}{\pi^2}\sum_{j,l}(2l+1)(-1)^{j+l+1+m_\alpha-m_\beta+j_\alpha-j_\beta+j_\gamma-j_\delta}\left[I^{(\omega)}_{\alpha\beta l}(r,r') \quad I^{(\sigma)}_{\alpha\beta l}(r,r')\right]$$

$$\times\ [(2l_\alpha+1)(2l_\gamma+1)(2j_\beta+1)(2j_\delta+1)]^{1/2}\,\langle l_\alpha 0 l 0 \mid l l_\beta 0\rangle\langle l_\gamma 0 l 0 \mid l l_\delta 0\rangle$$

$$\times\ (2j+1)\langle j m_\alpha - m_\beta j_\alpha m_\beta \mid j j_\beta j_\alpha m_\alpha\rangle\langle j - m_\alpha + m_\delta j_\delta m_\delta \mid j j_\delta j_\alpha m_\alpha\rangle$$

$$\times\ \begin{Bmatrix} l_\alpha & l_\beta & l \\ \frac{1}{2} & \frac{1}{2} & 1 \\ j_\alpha & j_\beta & j \end{Bmatrix} \begin{Bmatrix} l_\gamma & l_\delta & l \\ \frac{1}{2} & \frac{1}{2} & 1 \\ j_\gamma & j_\delta & j \end{Bmatrix}, \tag{29}$$

where

$$I^{(i)}_{\alpha\beta l}(r,r') = -\frac{\pi p^{(i)}_{\alpha\beta}}{4}\left[h^{(1)}_l(ip^{(i)}_{\alpha\beta}r)h^{(1)}_l(ip^{(i)}_{\alpha\beta}r') + h^{(1)}_l(ip^{(i)}_{\alpha\beta}r_>)h^{(2)}_l(ip^{(i)}_{\alpha\beta}r_<)\right], \tag{30}$$

with

$$p^{(i)}_{\alpha\beta} = \left[m_{(i)}{}^2 - (\epsilon_\alpha - \epsilon_\beta)^2\right]^{\frac{1}{2}}, \qquad i = \omega, \rho. \tag{31}$$

What remains is a double integral over $|\mathbf{x}| = r$ and $|\mathbf{y}| = r'$ which has to be done numerically:

$$\begin{aligned} H_{\rho\omega} = -\frac{\lambda g_\rho g_\omega}{m_\omega^2 - m_\rho^2}\int dr\,dr' \sum_{\alpha\beta\gamma\delta}\Big[& G_\alpha(r)G_\beta(r)J_{\alpha\beta\gamma\delta}(r,r')G_\gamma(r')G_\delta(r') \\ + & G_\alpha(r)G_\beta(r)J_{\alpha\beta,-\gamma-\delta}(r,r')F_\gamma(r')G_\delta(r') \\ + & F_\alpha(r)F_\beta(r)J_{-\alpha-\beta\gamma\delta}(r,r')G_\gamma(r')G_\delta(r') \\ + & G_\alpha(r)F_\beta(r)J_{\alpha-\beta\gamma-\delta}(r,r')G_\gamma(r')F_\delta(r') \\ - & G_\alpha(r)F_\beta(r)J_{\alpha-\beta-\gamma\delta}(r,r')F_\gamma(r')G_\delta(r') \\ - & F_\alpha(r)G_\beta(r)J_{-\alpha\beta\gamma-\delta}(r,r')G_\gamma(r')F_\delta(r') \\ + & F_\alpha(r)G_\beta(r)J_{-\alpha\beta-\gamma\delta}(r,r')F_\gamma(r')G_\delta(r') \\ + & F_\alpha(r)F_\beta(r)J_{-\alpha-\beta-\gamma-\delta}(r,r')F_\gamma(r')F_\delta(r')\Big] \\ \times\ & \tau_\gamma\,\delta_{\tau_\alpha\tau_\beta}\,\delta_{\tau_\gamma\tau_\delta}\,A^\dagger_\alpha A^\dagger_\gamma A_\delta A_\beta\,, \end{aligned} \tag{32}$$

where $-\alpha = \{n, -\kappa, m, t\}$.

Table 3 summarizes the results. Columns DME and SkII are the calculations of the NSA of Sato [17]. Column BI are the results of Blunden and Iqbal, as rescaled by Miller [7] to take into account the present value of the mixing. Column NR presents the results obtained with the Nedjadi-Rook wave functions, and columns H, HF, and T are the results obtained using the different approximations to the Walecka model (see Table 2). In the Table, only those levels which are bound are presented. We used for the mixing parameter the value $\lambda = -4500$ MeV^2. The masses and coupling constants of the ρ and the ω mesons used in calculating $\Delta_{\rho\omega}$ are the ones of the Bonn potential [15] in the case of the NR model, whereas for the Walecka model we have used the same values used in the calculation of the bound-state functions.

Both the Nedjadi-Rook and Walecka models give similar results. One notices two main features of the relativistic results: (1) they are of the same order, with a tendency of being on the average larger, than the nonrelativistic results of Blunden and Iqbal, and (2) the $p_{3/2}$ value is larger than the $p_{1/2}$ one for $A = 15$ nucleus, contrary to the BI result and to what is required to eliminate the anomaly. This last effect can be due to the core polarization; the missing nucleon can induce a large deformation of the strong scalar and vector fields. This is being investigated in the framework of a deformed mean field approximation in the Walecka model [18].

An important issue that is being discussed in the literature lately is the off-shell variation of the $\rho^0 - \omega$ mixing amplitude [19]. In the calculations in this paper, and in others involving CSB NN processes [3], one assumes that $<\rho^0|H|\omega>$ is weakly momentum dependent and uses the value extracted at the ω pole from data on $e^+e^- \to \rho, \omega \to \pi^+\pi^-$. However, while in the NN processes the exchanged mesons have spacelike momentum, in the e^+e^- processes they have timelike momentum. All of the studies in Ref. [19] predicted a significant momentum dependence for $<\rho^0|H|\omega>$ and a node near or at the origin ($q^2 = 0$). The implications of this is that the contribution of the mixing for the CSB component of NN force is very small and its importance to the NSA is significantly diminished. Although this is still controversial, as discussed by Miller and van Oers in

a recent review [20], the diminishing of the $\rho^0 - \omega$ mixing contribution might require new CSB effects for explaining the NSA. One class of effects that has received some attention lately is the one related to possible changes of the $u-$, $d-$quark condensates in medium [21].

Future investigations involve the study of core polarization effects [18], which might be important in presence of deformed strong scalar and vector mean fields, and the effects of the change of quark condensates in medium [21] in conjunction with the $\rho^0 \quad \omega$ mixing. The use of a deformed mean field approach will allow a complete study of all mirror nuclei and other analog states.

This work was partially supported by CNPq.

References

[1] J.A. Nolen and J.P. Schiffer, Annu. Rev. Nucl. Sci. 19 (1969) 414.

[2] K. Okamoto, Phys. Lett. 11 (1964) 150.

[3] G.A. Miller, B.M.K. Nefkens and I. Slaus, Phys. Rep. 194 (1990) 1.

[4] E.M. Henley and G.A. Miller, in: Mesons in nuclei, Vol. 1, eds. M. Rho and D.H. Wilkinson (North-Holland, Amsterdam, 1977).

[5] P. Langacker and D.A. Sparrow, Phys. Rev. Lett. 43 (1979) 1559; Phys. Rev. C 25 (1982) 1194; S.A. Coon and M.D. Scadron, Phys. Rev. C 26 (1982) 562; P.C. McNamee, M.D. Scadron and S.A. Coon, Nucl. Phys. A 249 (1975) 483.

[6] P.G. Blunden and M.J. Iqbal, Phys. Lett. B 198 (1987) 14.

[7] G.A. Miller, Nucl. Phys. A 518 (1989) 345.

[8] B.D. Serot and J.D. Walecka, Adv. Nucl. Phys. 16 (1983) 1.

[9] Y. Nedjadi and J.R. Rook, Nucl. Phys. A 484 (1985) 525.

[10] G. Krein, D.P. Menezes and M. Nielsen, Phys. Lett. B 294 (1992) 7.

[11] C.J. Horowitz, D.P. Murdoch, and B.D. Serot, Computational Nuclear Physics I, ed. K. Langanke, J.A. Maruhn, S.E. Koonin (Springer Verlag, 1993).

[12] D. Vautherin e D.M. Brink, Phys. Rev. C (1972) 626.

[13] L. Ray e P.E. Hodgson, Phys. Rev. C 20 (1979) 2403.

[14] H.F. Boersma e R. Malfliet, Phys. Rev. C **49**, 1495 (1994).

[15] R. Machleidt, Adv. Nucl. Phys. **19**, (1989) 189.

[16] C.J. Horowitz and B.D. Serot, Nucl.Phys. A 368 (1981) 503.

[17] H. Sato, Nucl.Phys. A 269 (1976) 378.

[18] L.A. Barreiro, W. Köepf and G. Krein, work in progress.

[19] T. Goldman, J.A. Hendersen and A.W. Thomas, Few Body Systems 12 (1992) 123; G. Krein, A.W. Thomas and A.G. Williams, Phys. Lett. B 317 (1993) 293; J. Piekarewicz and A.G. Williams, Phys. Rev. C 47 (1993) R2461; T. Hatsuda, E.M. Henley, Th. Meissner and G. Krein, Phys. Rev. C 49 (1994) 452; K.L. Mitchell, P.C. Tandy, C.D. Roberts and R.T. Cahill, Phys. Lett. B 335 (1994) 282.

[20] G.A. Miller and W.T.H van Oers, "Charge Independence and Charge Symmetry," nucl-th/9409013.

[21] E.M. Henley and G. Krein, Phys. Rev. Lett. 62 (1989) 2586; K. Saito and A.W. Thomas, Phys. Lett. B 335 (1994) 17.

Table 1: Single-particle energies (in MeV) and r.m.s. charge radii (in fm) for the Nedjadi-Rook model. The upper (lower) part is for ^{16}O (^{40}Ca).

	NR		Exp	
	p	n	p	n
$1s_{1/2}$	-38.241	-42.515	-40.± 8	
$1p_{3/2}$	-18.293	-22.211	-18.4	-21.8
$1p_{1/2}$	-11.408	-15.263	-12.1	-15.7
$1d_{5/2}$	-1.030	-4.414	-0.6	-4.17
$2s_{1/2}$	0.000	-3.531	-0.1	-3.27
$\langle r^2\rangle^{1/2}$	2.65	2.60	2.73	
$1s_{1/2}$	-46.402	-54.473	-48.5±5.0	
$1p_{3/2}$	-30.655	-38.322	-36.0±3.0	
$1p_{1/2}$	-26.504	-34.192	-31.5±3.5	
$1d_{5/2}$	-15.481	-22.709	-16.0±2.0	
$2s_{1/2}$	-10.224	-17.268	-12.0±1.0	-18.1
$1d_{3/2}$	-9.347	-16.505	-8.5±2.0	-15.6
$1f_{7/2}$	-1.661	-8.279	-1.4	-8.36
$\langle r^2\rangle^{1/2}$	3.46	3.39	3.49	

Table 2: Single-particle energies (in MeV) and r.m.s. charge radii (in fm) for the Walecka model. The upper (lower) part is for ^{16}O (^{40}Ca).

	H		HF		T		Exp	
	p	n	p	n	p	n	p	n
$1s_{1/2}$	-39.251	-43.493	-39.187	-43.429	-39.132	-43.553	-40.±8	
$1p_{3/2}$	-18.464	-22.379	-18.433	-22.349	-18.271	-22.409	-18.4	-21.8
$1p_{1/2}$	-9.792	-13.586	-9.786	-13.570	-9.543	-13.557	-12.1	-15.7
$1d_{5/2}$	-1.127	-4.651	-1.121	-4.643	-0.869	-4.621	-0.6	-4.17
$\langle r^2\rangle^{1/2}$	2.687	2.658	2.691	2.659	2.692	2.659	2.73	--
$1s_{1/2}$	-51.160	-59.535	-51.076	-59.447	-50.904	-59.644	-48.5±5.0	--
$1p_{3/2}$	-34.787	-42.791	-34.637	-42.639	-34.429	-42.886	-36.0±3.0	--
$1p_{1/2}$	-28.735	-36.763	-28.606	-36.738	-28.309	-36.801	-31.5±3.5	--
$1d_{5/2}$	-18.497	-26.125	-18.366	-26.084	-18.001	-26.181	-16.0±2.0	--
$2s_{1/2}$	-9.045	-16.478	-9.008	-16.344	-8.760	-16.421	12.0±1.0	-18.1
$1d_{3/2}$	-8.836	-15.957	-8.705	-15.828	-8.105	-15.930	-8.5±2.0	-15.6
$1f_{7/2}$	-3.169	-10.350	-3.003	-10.362	-2.441	-10.374		-8.36
$\langle r^2\rangle^{1/2}$	3.45	3.39	3.47	3.40	3.43	3.39	3.49	--

Table 3: $\Delta E_{\rho\omega}$ (keV)

		Required CSB		$\rho^0 - \omega$				
A	State	DME	SkII	BI	NR	H	HF	T
15	$1p_{3/2}^{-1}$	250	190	182	191	208	209	209
	$1p_{1/2}^{-1}$	380	290	227	188	203	204	204
17	$1d_{5/2}$	300	190	131	168	166	166	166
39	$2s_{1/2}^{-1}$	370	270	290	220	232	232	232
	$1d_{3/2}^{-1}$	540	430	281	336	335	336	337
41	$1f_{7/2}$	440	350	175	268	260	261	262